

# Thermal buckling analysis of skew fibre-reinforced composite and sandwich plates using shear deformable finite element models

T. Kant<sup>\*</sup>, C.S. Babu

*Department of Civil Engineering, Indian Institute of Technology Bombay, Powai, Mumbai 400 076, India*

## Abstract

The paper considers the elastic buckling of skew fibre-reinforced composite and sandwich plates subjected to thermal loads. To the best of the authors' knowledge, there is no paper in the open literature on this subject and the present paper attempts to fill this gap. Two shear deformable finite element models, one based on first-order shear deformation theory and the other based on higher-order shear deformation theory, are employed to obtain thermal buckling solutions. Extensive numerical results are presented for both thin and thick laminated composite plates with various skew angles, lamination parameters and boundary conditions. A few results for skew sandwiches are obtained for various geometric parameters and skew angles. Results presented, not available so far, could be useful to designers and researchers who may use them as benchmark values to validate their numerical techniques and software for similar problems. © 2000 Elsevier Science Ltd. All rights reserved.

*Keywords:* Buckling; Higher-order theory; Shear deformation; Skew plate; Skew laminates; Skew sandwiches; Thermal buckling

## 1. Introduction

Fibre-reinforced composite materials due to their high specific strength and stiffness are becoming increasingly used in many engineering applications, especially in the aerospace and ship building industries. It is well known that skew or oblique plates made of these materials are important structural components of ship hulls and swept wings of aeroplanes. Buckling is one of the primary modes of failure of these elements when they are subjected to membrane stresses caused by either thermal loads or mechanical loads or a combination of these loads. Thus the buckling strength of skew composite laminates is one of the factors governing their design and its accurate determination is of interest to designers.

Considerable research [1–4] has been published investigating the buckling response of skew composite laminates. In these investigations, numerical methods such as the finite element method, the Rayleigh–Ritz method, etc. are used as exact solutions cannot be obtained due to the use of a non-orthogonal coordinate system in the derivation of the governing differential equations. Reddy and Palaninathan [1] have employed a

triangular finite element based on classical laminated plate theory. Jaunky et al. [2] and Wang [3] have used the Rayleigh–Ritz method incorporating first-order shear deformation effects. Very recently, Babu and Kant [4] have presented two  $C^0$  shear deformable finite element formulations for the buckling analysis of skew laminated composite and sandwich panels. A 16-node bi-cubic Lagrange element is used in the formulations. In all these investigations, skew laminates subjected to only mechanical loads are considered. Surprisingly, in the case of skew composite laminated and sandwich plates subjected to thermal loads, there are virtually no papers in the open literature; although there are a few studies [5–7] on thermal buckling of isotropic skew plates.

The objective of this work is to fill this gap by presenting a study of the thermal buckling of skew laminated composite and sandwich plates. The two shear deformable finite element models presented by the authors [4] previously for mechanical buckling analyses are employed here for thermal buckling analyses. One of these models is based on Reissner–Mindlin first-order theory and the other is based on a higher-order theory developed by Kant and his fellow researchers [8–10]. The accuracy of the models is verified against the literature values for isotropic skew plates. New results are presented for skew laminated composite and sandwich plates using the standard material properties available in the literature.

<sup>\*</sup> Corresponding author.

*E-mail addresses:* tkant@civil.iitb.ernet.in (T. Kant), rssh@civil.iitb.ernet.in (C.S. Babu).

## 2. Theoretical formulation

The two shear deformation theories considered for investigation in the present work are based on the assumption of the displacement fields in the following form:

(a) First-order shear deformation theory (FSDT), 5 degrees of freedom/node

$$\begin{aligned} u(x, y, z) &= u_0(x, y) + z\theta_y(x, y), \\ v(x, y, z) &= v_0(x, y) - z\theta_x(x, y), \\ w(x, y, z) &= w_0(x, y). \end{aligned} \quad (1)$$

(b) Higher-order shear deformation theory (HSDT), 9 degrees of freedom/node

$$\begin{aligned} u(x, y, z) &= u_0(x, y) + z\theta_y(x, y) + z^2u_0^*(x, y) + z^3\theta_y^*(x, y), \\ v(x, y, z) &= v_0(x, y) - z\theta_x(x, y) + z^2v_0^*(x, y) - z^3\theta_x^*(x, y), \\ w(x, y, z) &= w_0(x, y), \end{aligned} \quad (2)$$

where  $u$ ,  $v$  and  $w$  define the displacements of any generic point  $(x, y, z)$  in the plate space,  $u_0$ ,  $v_0$  and  $w_0$  denote the displacements (Fig. 1) of a point  $(x, y)$  on the middle plane,  $\theta_x$  and  $\theta_y$  are the rotations of normal to middle-plane about  $x$ - and  $y$ -axes, respectively. The parameters  $u_0^*$ ,  $v_0^*$ ,  $\theta_x^*$  and  $\theta_y^*$  are higher-order terms in the Taylor series expansion and are also defined at the mid-surface.

Neglecting the transverse stress ( $\sigma_z$ ) and strain ( $\varepsilon_z$ ), the Duhamel–Neumann form of Hooke's law for the  $L^{\text{th}}$  lamina in the laminate co-ordinates  $(x, y, z)$  is written as

$$\begin{Bmatrix} \sigma_x \\ \sigma_y \\ \tau_{xy} \\ \tau_{yz} \\ \tau_{xz} \end{Bmatrix} = \begin{bmatrix} Q_{11} & Q_{12} & Q_{13} & 0 & 0 \\ Q_{12} & Q_{22} & Q_{23} & 0 & 0 \\ Q_{13} & Q_{23} & Q_{33} & 0 & 0 \\ 0 & 0 & 0 & Q_{44} & Q_{45} \\ 0 & 0 & 0 & Q_{45} & Q_{55} \end{bmatrix} \begin{Bmatrix} \varepsilon_x - \alpha_x \Delta T \\ \varepsilon_y - \alpha_y \Delta T \\ \gamma_{xy} - \alpha_{xy} \Delta T \\ \gamma_{yz} \\ \gamma_{xz} \end{Bmatrix} \quad (3)$$

or in short form

$$\boldsymbol{\sigma} = \mathbf{Q}(\boldsymbol{\varepsilon} - \boldsymbol{\varepsilon}_t) \quad (4)$$

in which

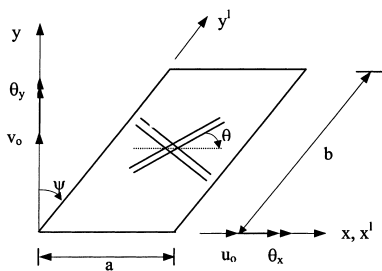


Fig. 1. The geometry of skew laminate.

$$\begin{aligned} \boldsymbol{\sigma} &= \{\sigma_x \ \sigma_y \ \tau_{xy} \ \tau_{yz} \ \tau_{xz}\}^T, \\ \boldsymbol{\varepsilon} &= \{\varepsilon_x \ \varepsilon_y \ \gamma_{xy} \ \gamma_{yz} \ \gamma_{xz}\}^T, \\ \boldsymbol{\varepsilon}_t &= \{\alpha_x \ \alpha_y \ \alpha_{xy} \ 0\}^T \Delta T \end{aligned} \quad (5)$$

are respectively the stress, the total strain and the thermal strain vectors. The  $Q_{ij}$ 's are the plane stress reduced stiffness coefficients. The transformation of the stresses/strains between the lamina and laminate co-ordinate systems follows the usual stress tensor transformation rule.  $\Delta T$  is temperature rise. The  $\alpha_x$ ,  $\alpha_y$  and  $\alpha_{xy}$  terms are defined as follows:

$$\begin{aligned} \alpha_x &= \alpha_1 \cos^2 \theta + \alpha_2 \sin^2 \theta, \\ \alpha_y &= \alpha_1 \sin^2 \theta + \alpha_2 \cos^2 \theta, \\ \alpha_{xy} &= 2(\alpha_1 - \alpha_2) \sin \theta \cos \theta, \end{aligned} \quad (6)$$

where  $\alpha_1$  and  $\alpha_2$  are the thermal expansion coefficients of the lamina along the longitudinal and transverse directions of the fibres, respectively. It will be noted that the theoretical formulation given in the rest of the paper is based on HSDT and the formulation corresponding to FSDT can be obtained from that of HSDT by truncating the terms corresponding to the higher-order displacement degrees of freedom.

Substituting Eq. (2) into Green's strain tensor [11], with  $\varepsilon_z = 0$ , the generalized strain vector components are obtained as:

$$\begin{aligned} \varepsilon_x &= \varepsilon_x^0 + z\chi_x^0 + z^2 \varepsilon_x^* + z^3 \chi_x^* + z^4 \varepsilon_x^{**} + z^5 \chi_x^{**} + z^6 \varepsilon_x^{***}, \\ \varepsilon_y &= \varepsilon_y^0 + z\chi_y^0 + z^2 \varepsilon_y^* + z^3 \chi_y^* + z^4 \varepsilon_y^{**} + z^5 \chi_y^{**} + z^6 \varepsilon_y^{***}, \\ \gamma_{xy} &= \varepsilon_{xy}^0 + z\chi_{xy}^0 + z^2 \varepsilon_{xy}^* + z^3 \chi_{xy}^* + z^4 \varepsilon_{xy}^{**} + z^5 \chi_{xy}^{**} + z^6 \varepsilon_{xy}^{***}, \\ \gamma_{yz} &= \phi_y^0 + z\psi_y^0 + z^2 \phi_y^* + z^3 \psi_y^* + z^4 \phi_y^{**} + z^5 \psi_y^{**}, \\ \gamma_{xz} &= \phi_x^0 + z\psi_x^0 + z^2 \phi_x^* + z^3 \psi_x^* + z^4 \phi_x^{**} + z^5 \psi_x^{**}. \end{aligned} \quad (7)$$

Note that the five generalized strain components are expressed in terms of 33 mid-surface strain components denoted by the vector,  $\bar{\boldsymbol{\varepsilon}}$ . Each of the components of the strain vector,  $\bar{\boldsymbol{\varepsilon}}$  has both linear ( $\bar{\boldsymbol{\varepsilon}}_0$ ) as well as non-linear parts ( $\bar{\boldsymbol{\varepsilon}}_L$ ) which are expressed in terms of mid-plane displacement components (see Appendix A).

In the absence of external loads, the total potential energy of the laminate for the thermal buckling problem is expressed as

$$\Pi = \frac{1}{2} \int_v \{\boldsymbol{\varepsilon}_0 - \boldsymbol{\varepsilon}_t\}^T \boldsymbol{\sigma} dv + \int_v \boldsymbol{\varepsilon}_L^T \boldsymbol{\sigma} dv, \quad (8)$$

where  $\boldsymbol{\varepsilon}_0$  and  $\boldsymbol{\varepsilon}_L$  are respectively the linear and non-linear parts of the generalized strain vector,  $\boldsymbol{\varepsilon}$ . The second expression in the above equation is the work done by initial (or prebuckling) stresses. Substituting for  $\boldsymbol{\varepsilon}_0$ ,  $\boldsymbol{\varepsilon}_L$  and  $\boldsymbol{\sigma}$  in Eq. (8) and performing an explicit integration through the laminate thickness, the potential energy of the laminate is rewritten as

$$\Pi = \frac{1}{2} \int_A \bar{\boldsymbol{\varepsilon}}_0^T \mathbf{D} \bar{\boldsymbol{\varepsilon}}_0 dA + \int_A \bar{\boldsymbol{\varepsilon}}_L^T \bar{\boldsymbol{\sigma}} dA - \int_A \bar{\boldsymbol{\varepsilon}}_0^T \bar{\boldsymbol{\sigma}}_t dA - f(Q_{ij}, \alpha_i) \quad (9)$$

in which  $f$  is a function of  $Q_{ij}$  and  $\alpha_i$ , and the new vectors in concise form are expressed as

$$\bar{\boldsymbol{\sigma}} = \{\mathbf{N}^T \mathbf{M}^T \mathbf{Q}^T\}^T \quad \text{and} \quad \bar{\boldsymbol{\sigma}}_t = \{\mathbf{N}_t^T \mathbf{M}_t^T \mathbf{O}_t^T\}^T, \quad (10)$$

where

$$\begin{aligned} \mathbf{N} &= \{N_x^0, N_y^0, N_{xy}^0, N_x^*, N_y^*, N_{xy}^*, N_x^{**}, N_y^{**}, N_{xy}^{**}, N_x^{***}, N_y^{***}, N_{xy}^{***}\}^T, \\ \mathbf{M} &= \{M_x^0, M_y^0, M_{xy}^0, M_x^*, M_y^*, M_{xy}^*, M_x^{**}, M_y^{**}, M_{xy}^{**}\}^T, \\ \mathbf{Q} &= \{Q_x^0, Q_y^0, S_x^0, S_y^0, Q_x^*, Q_y^*, S_x^*, S_y^*, Q_x^{**}, Q_y^{**}, S_x^{**}, S_y^{**}\}^T, \\ \mathbf{N}_t &= \{N_{tx}^0, N_{ty}^0, N_{txy}^0, N_{tx}^*, N_{ty}^*, N_{txy}^*, N_{tx}^{**}, N_{ty}^{**}, N_{txy}^{**}, N_{tx}^{***}, N_{ty}^{***}, N_{txy}^{***}\}^T, \\ \mathbf{M}_t &= \{M_{tx}^0, M_{ty}^0, M_{txy}^0, M_{tx}^*, M_{ty}^*, M_{txy}^*, M_{tx}^{**}, M_{ty}^{**}, M_{txy}^{**}\}^T, \\ \mathbf{O}_t &= \{0, 0, 0, 0, 0, 0, 0, 0, 0, 0, 0, 0\}^T. \end{aligned}$$

The components of stress resultant and stress couple vectors in Eq. (10) are defined as follows:

$$\begin{bmatrix} N_x^0 & N_y^0 & N_{xy}^0 \\ N_x^* & N_y^* & N_{xy}^* \\ N_x^{**} & N_y^{**} & N_{xy}^{**} \\ N_x^{***} & N_y^{***} & N_{xy}^{***} \end{bmatrix} = \sum_{L=1}^{NL} \int_{Z_L}^{Z_{L+1}} \begin{bmatrix} 1 \\ z^2 \\ z^4 \\ z^6 \end{bmatrix} [\sigma_x \quad \sigma_y \quad \tau_{xy}] dz, \quad (11)$$

$$\begin{bmatrix} M_x^0 & M_y^0 & M_{xy}^0 \\ M_x^* & M_y^* & M_{xy}^* \\ M_x^{**} & M_y^{**} & M_{xy}^{**} \end{bmatrix} = \sum_{L=1}^{NL} \int_{Z_L}^{Z_{L+1}} \begin{bmatrix} z \\ z^3 \\ z^5 \end{bmatrix} [\sigma_x \quad \sigma_y \quad \tau_{xy}] dz, \quad (12)$$

$$\begin{bmatrix} Q_x^0 & Q_y^0 \\ S_x^0 & S_y^0 \\ Q_x^* & Q_y^* \\ S_x^* & S_y^* \\ Q_x^{**} & Q_y^{**} \\ S_x^{**} & S_y^{**} \end{bmatrix} = \sum_{L=1}^{NL} \int_{Z_L}^{Z_{L+1}} \begin{bmatrix} 1 \\ z \\ z^2 \\ z^3 \\ z^4 \\ z^5 \end{bmatrix} [\tau_{xz} \quad \tau_{yz}] dz, \quad (13)$$

$$\mathbf{N}_t = \sum_{L=1}^{NL} \begin{bmatrix} Q_{ij} H_1 \\ Q_{ij} H_3 \\ Q_{ij} H_5 \\ Q_{ij} H_7 \end{bmatrix} \begin{Bmatrix} \alpha_x \\ \alpha_y \\ \alpha_{xy} \end{Bmatrix} \Delta T$$

and

$$\mathbf{M}_t = \sum_{L=1}^{NL} \begin{bmatrix} Q_{ij} H_2 \\ Q_{ij} H_4 \\ Q_{ij} H_6 \end{bmatrix} \begin{Bmatrix} \alpha_x \\ \alpha_y \\ \alpha_{xy} \end{Bmatrix} \Delta T, \quad (14)$$

where

$$i, j = 1, 2, 3 \quad \text{and} \quad H_i = \frac{(z_{L+1}^i - z_L^i)}{i}$$

After integration, the stress resultants in Eqs. (11)–(13) are written in matrix form as

$$\bar{\boldsymbol{\sigma}} = \mathbf{D} \bar{\boldsymbol{\varepsilon}} - \bar{\boldsymbol{\sigma}}_t, \quad (15)$$

where

$$\mathbf{D} = \begin{bmatrix} \mathbf{D}_M & \mathbf{D}_C & 0 \\ \mathbf{D}_C^T & \mathbf{D}_B & 0 \\ 0 & 0 & \mathbf{D}_S \end{bmatrix} \quad (16)$$

in which  $\mathbf{D}_M$ ,  $\mathbf{D}_B$ ,  $\mathbf{D}_C$  and  $\mathbf{D}_S$  are the membrane, flexural, membrane–flexural coupling and shear rigidity matrices, respectively. The components of the rigidity matrix are given in Appendix A.

Following the standard procedure of the finite element formulation and the transformation of the stiffness matrices and the load vector from global axes  $x - y$  to local axes  $x^1 - y^1$  (Fig. 1) as explained in Ref. [4], the equilibrium and stability conditions are obtained as

$$\mathbf{K}_0 \bar{\mathbf{d}} = \mathbf{R}, \quad (17)$$

$$[\mathbf{K}_0 + \lambda \mathbf{K}_g] \delta \bar{\mathbf{d}} = 0, \quad (18)$$

where  $\mathbf{K}_0$ ,  $\mathbf{K}_g$  and  $\mathbf{R}$  are the linear stiffness matrix, the geometric stiffness matrix and the thermal load vector, respectively.  $\bar{\mathbf{d}}$  is the nodal displacement vector of the plate.

### 2.1. Thermal buckling analysis

The calculation of the critical buckling temperature consists of two stages. For a specified rise in temperature ( $\Delta T$ ), a linear static analysis (17) is carried out to determine the thermal stress resultants. These stress resultants are then used to compute the geometric stiffness matrix which is subsequently used in Eq. (18) to determine the smallest eigenvalue,  $\lambda$  and the associated mode shape,  $\delta \bar{\mathbf{d}}$ . The critical temperature,  $T_{cr}$  of the plate is calculated using

$$T_{cr} = \lambda \Delta T. \quad (19)$$

### 3. Numerical results and discussion

Computer programs have been developed, based on the foregoing finite element models, to solve a number of thermal buckling examples of skew composite laminated and sandwich plates. The programs can handle panels subjected to non-uniform temperature rise over the surface and through the thickness. However, in all the examples considered here, the temperature rise is assumed to be uniform. In general a  $6 \times 6$  skew mesh of 16-node elements has been used in the computations except for the convergence study presented on isotropic plate. The selective integration scheme, namely  $4 \times 4$  Gauss–Legendre for the membrane, flexure, membrane–flexure and  $3 \times 3$  for the shear energy contributions was used for thin plates (side to thickness ratio  $(a/h) > 20$ ) and a full  $(4 \times 4)$  integration scheme is used for thick

Table 1  
Critical temperature parameter,  $\lambda_T^*$  for clamped isotropic skew plates

$\Psi$	Mesh	Ref. [7]	HSDT		FSDT	
			FI	SI	FI	SI
0°	6 × 6	3.71	3.714	3.710	3.714	3.710
15°	6 × 6	3.95	3.952	3.946	3.952	3.946
30°	6 × 6	4.80	4.815	4.795	4.815	4.795
45°	3 × 3	–	7.799	6.938	7.799	6.938
	4 × 4	–	7.294	6.927	7.293	6.927
	5 × 5	–	7.105	6.922	7.105	6.922
	6 × 6	6.92	7.015	6.919	7.014	6.919

laminates. All of the laminates considered were assumed to have an aspect ratio of  $a/b = 1$ , though the general case  $a \neq b$  may also be studied without any difficulty. In all of the FSDT model computations, a shear correction factor of  $5/6$  was used.

Due to the lack of comparative results for skew composite laminated plates, the accuracy of the present formulations was evaluated only with respect to results for isotropic plates. Subsequently, some new results are presented for laminated composite and sandwich skew plates.

### 3.1. Isotropic skew plates

Critical buckling temperature values of clamped isotropic skew plates are given by Prabhu and Durvasula [7]. They used classical plate theory in conjunction with the Ritz method. To obtain the classical plate theory solution, a thin plate with  $a/h = 1000$  is analysed here. The critical temperature values are evaluated in non-dimensional form, expressed as  $\lambda_T^* = E\alpha b^2 h T_{cr} / \pi^2 D$  where  $T_{cr}$  is the critical temperature,  $\alpha$  the thermal expansion coefficient,  $E$  the Young's Modulus and  $D = Eh^3/12(1 - \nu^2)$ . Poisson's ratio,  $\nu$  is 0.3. The results obtained with full integration (FI) and selective integration (SI) schemes are given in Table 1 for four skew angles,  $\Psi = 0^\circ, 15^\circ, 30^\circ$  and  $45^\circ$ . For  $\Psi = 45^\circ$ , the re-

sults obtained with successive refined meshes are also presented. The results of the present models obtained with the SI scheme are almost identical with the results given in [7] and the difference between the two integration schemes is negligible. Thus, the results demonstrate that the 16-node element is less susceptible to shear locking even in a distorted mesh. It is noted that the element exhibits monotonic convergence and a  $6 \times 6$  skew mesh is considered adequate for further analysis.

### 3.2. Composite skew laminates

Cross-ply and angle-ply laminates are considered. The lamination schemes used are: (i) symmetric cross-ply ( $0^\circ/90^\circ/90^\circ/0^\circ$ ) and (ii) anti-symmetric angle-ply ( $45^\circ/-45^\circ/\dots$ ) with the number of layers,  $NL = 4$  and 10. Both thin and thick skew laminates with four different edge conditions are analysed. The edge conditions considered are: (i) all edges simply supported (SSSS), (ii) straight edges clamped and skewed edges simply supported (CSCS), (iii) straight edges simply supported and skewed edges clamped (SCSC) and (iv) all edges clamped (CCCC). The simply supported (SS2) and clamped boundary conditions used here are given in Ref. [4]. The skew angle,  $\Psi$  is varied from  $0^\circ$  to  $45^\circ$ . The material characteristics [12] of individual lamina used here are:

Table 2  
Critical temperature parameter ( $\lambda_T 10^2$ ) of symmetric cross-ply  $[(0^\circ/90^\circ)_s]$  skew laminate with various edge conditions ( $a/h = 100$ ) [ $6 \times 6$  mesh]

$\Psi$	Theory	Edge conditions			
		SSSS	CSCS	SCSC	CCCC
0°	HSDT	0.0996	0.1440	0.2530	0.3348
	FSDT	0.0997	0.1441	0.2532	0.3352
15°	HSDT	0.1017	0.1514	0.2606	0.3441
	FSDT	0.1018	0.1515	0.2608	0.3444
30°	HSDT	0.1116	0.1794	0.2916	0.3572
	FSDT	0.1118	0.1797	0.2919	0.3576
45°	HSDT	0.1427	0.2507	0.3295	0.4169
	FSDT	0.1432	0.2516	0.3298	0.4174

Table 3  
Critical temperature parameter ( $\lambda_T 10^2$ ) of anti-symmetric angle-ply ( $45^\circ/-45^\circ/...$ ) skew laminates with various edge conditions ( $a/h = 100$ ) [ $6 \times 6$  mesh]

NL	$\psi$	Theory	Edge conditions			
			SSSS	CSCS	SCSC	CCCC
4	0°	HSDT	0.1468	0.2322	0.2322	0.3036
		FSDT	0.1469	0.2324	0.2324	0.3040
	15°	HSDT	0.1492	0.2374	0.2517	0.3248
		FSDT	0.1494	0.2377	0.2520	0.3252
	30°	HSDT	0.1649	0.2652	0.3174	0.3980
		FSDT	0.1651	0.2657	0.3178	0.3986
	45°	HSDT	0.2171	0.3534	0.4629	0.5680
		FSDT	0.2174	0.3541	0.4637	0.5691
10	0°	HSDT	0.1675	0.2637	0.2637	0.3441
		FSDT	0.1675	0.2637	0.2637	0.3442
	15°	HSDT	0.1696	0.2689	0.2860	0.3683
		FSDT	0.1696	0.2690	0.2861	0.3684
	30°	HSDT	0.1850	0.2980	0.3609	0.4514
		FSDT	0.1851	0.2981	0.3610	0.4515
	45°	HSDT	0.2406	0.3938	0.5266	0.6441
		FSDT	0.2407	0.3940	0.5268	0.6443

Table 4  
Critical temperature parameter ( $\lambda_T$ ) of symmetric cross-ply  $[(0^\circ/90^\circ)_8]$  skew laminate with various edge conditions ( $a/h = 10$ ) [ $6 \times 6$  mesh]

$\psi$	Theory	Edge conditions			
		SSSS	CSCS	SCSC	CCCC
0°	HSDT	0.0757	0.1044	0.1305	0.1601
	FSDT	0.0770	0.1069	0.1344	0.1655
15°	HSDT	0.0767	0.1074	0.1340	0.1618
	FSDT	0.0784	0.1108	0.1383	0.1674
30°	HSDT	0.0821	0.1189	0.1447	0.1690
	FSDT	0.0849	0.1243	0.1491	0.1753
45°	HSDT	0.0985	0.1462	0.1523	0.1893
	FSDT	0.1031	0.1533	0.1577	0.1982

Table 5  
Critical temperature parameter ( $\lambda_T$ ) of anti-symmetric angle-ply ( $45^\circ/-45^\circ/...$ ) skew laminates with various edge conditions ( $a/h = 10$ ) [ $6 \times 6$  mesh]

NL	$\psi$	Theory	Edge conditions			
			SSSS	CSCS	SCSC	CCCC
4	0°	HSDT	0.1061	0.1360	0.1360	0.1609
		FSDT	0.1099	0.1422	0.1422	0.1688
	15°	HSDT	0.1056	0.1364	0.1427	0.1678
		FSDT	0.1098	0.1427	0.1496	0.1764
	30°	HSDT	0.1116	0.1451	0.1625	0.1886
		FSDT	0.1162	0.1518	0.1716	0.1995
	45°	HSDT	0.1341	0.1721	0.1950	0.2249
		FSDT	0.1399	0.1805	0.2078	0.2399
10	0°	HSDT	0.1208	0.1534	0.1534	0.1809
		FSDT	0.1215	0.1544	0.1544	0.1820
	15°	HSDT	0.1201	0.1537	0.1611	0.1887
		FSDT	0.1209	0.1546	0.1621	0.1899
	30°	HSDT	0.1256	0.1621	0.1835	0.2121
		FSDT	0.1265	0.1630	0.1847	0.2135
	45°	HSDT	0.1497	0.1909	0.2199	0.2526
		FSDT	0.1506	0.1918	0.2211	0.2542

$$E_1/E_2 = 15, E_3 = E_2, \quad G_{12}/E_2 = G_{13}/E_2 = 0.5000,$$

$$G_{23}/E_2 = 0.3356, \quad \nu_{12} = \nu_{13} = 0.3, \quad \nu_{23} = 0.49,$$

$$\alpha_1/\alpha_0 = 0.015, \quad \alpha_2/\alpha_0 = \alpha_3/\alpha_0 = 1.0,$$

where  $\alpha_0$  is a normalisation factor for the coefficient of thermal expansion.

Tables 2 and 3 show the critical temperature parameter,  $\lambda_T = \alpha_0 T_{cr}$  for symmetric cross-ply ( $0^\circ/90^\circ/90^\circ/0^\circ$ ) and anti-symmetric angle-ply ( $45^\circ/-45^\circ/\dots$ ) thin ( $a/h = 100$ ) skew laminates, respectively. As expected, the results of the first-order and higher-order theories show good agreement for all the edge conditions and for all the skew angles considered.

Tables 4 and 5 show the critical temperature parameter for thick ( $a/h = 10$ ) symmetric cross-ply ( $0^\circ/90^\circ/90^\circ/0^\circ$ ) and anti-symmetric angle-ply ( $45^\circ/-45^\circ/\dots$ ) laminates, respectively. It is clear that for both cross and angle-ply laminates, the first-order theory over-estimates the critical temperature and the difference between the two theories increases with increasing skew angle. The maximum difference between the two theories occurs with CCCC laminates when  $\Psi = 45^\circ$ . The difference is about 4.7% in the cross-ply laminate and in

the angle-ply laminate with  $NL = 4$ , the difference is about 6.7%. However, for the ten layered angle-ply laminate, the results of both theories are nearly the same with a maximum difference of about 1%. In general, the critical temperature of both the thin and thick laminates increases with skew angle. But the increase is more pronounced in thin laminates.

Figs. 2(a) and (b) show the effect of width-to-thickness ratio on the critical temperature of four-layered anti-symmetric angle-ply ( $45^\circ/-45^\circ/45^\circ/-45^\circ$ ) skew laminate for SSSS and CCCC support conditions, respectively. The results obtained with HSDT analysis are used here. The critical temperature parameter decreases, i.e., the effect of transverse shear deformation increases, with increase in laminate thickness. The effect of transverse shear deformation is seen to increase with increase in the skew angle for both simply supported and clamped laminates, but the increase is more significant in clamped skew laminates. The effect of skew angle on critical temperature decreases with increase in thickness and for thick laminates with  $a/h = 5$ , the skew angle has negligible influence on critical temperature.

### 3.3. Skew sandwiches

Symmetric skew sandwich panels with cross-ply composite face sheets and a honeycomb core are considered here. The stacking sequence of the panel is  $[(0^\circ/90^\circ)_5/\text{core}/(90^\circ/0^\circ)_5]$ . The material characteristics [13] of the face sheets and core are:

Face sheets

$$E_1/E_2 = 19, E_3 = E_2, \quad G_{12}/E_2 = 0.520,$$

$$G_{23}/E_2 = 0.338, \quad \nu_{12} = \nu_{13} = 0.32, \quad \nu_{23} = 0.49,$$

$$\alpha_1/\alpha_0 = 0.001, \quad \alpha_2/\alpha_0 = \alpha_3/\alpha_0 = 1.0.$$

Core

$$E_1/E_2^f = 3.2 \times 10^{-5}, \quad E_2/E_2^f = 2.9 \times 10^{-5}, \quad E_3/E_2^f = 0.4,$$

$$G_{12}/E_2^f = 2.4 \times 10^{-3}, \quad G_{13}/E_2^f = 7.9 \times 10^{-2},$$

$$G_{23}/E_2^f = 6.6 \times 10^{-2}, \quad \nu_{12} = 0.99,$$

$$\nu_{13} = \nu_{23} = 3 \times 10^{-5}, \quad \alpha_1 = \alpha_2 = \alpha_3 = 1.36\alpha_0,$$

where,  $E_2^f$  refers to the face sheets. Numerical results are presented in Table 6 for simply supported (SSSS) panels with  $\Psi = 0^\circ, 15^\circ, 30^\circ$  and  $45^\circ$ . Two parameters,  $a/h$  and  $h_f/h$  are varied, where  $h_f$  is thickness of each of the face sheets. For the validation of the present models, 3-D elasticity solution results [13,14] are also given for panels with  $\Psi = 0^\circ$ . It may be noted that the HSDT results match well with the 3-D elasticity solution for all values of  $h_f/h$ , whereas FSDT over-estimates the buckling temperature by a significant margin at higher values of  $h_f/h$ . In the case of skew panels, for all values of  $\Psi$  and  $a/h$  ratios considered, the FSDT and HSDT results are almost identical for

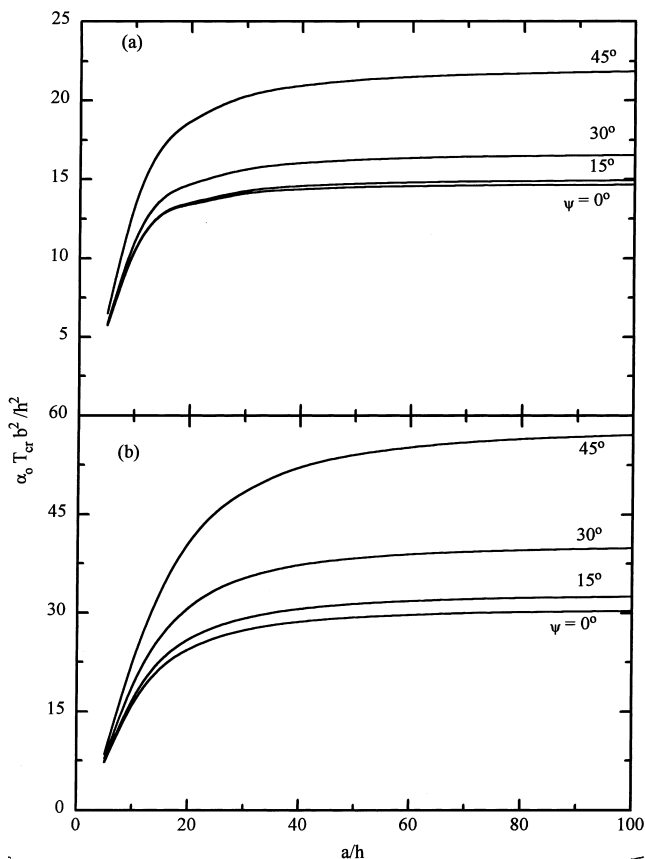


Fig. 2. Effect of thickness ratio on the critical temperature of anti-symmetric angle-ply ( $45^\circ/-45^\circ/45^\circ/-45^\circ$ ) skew laminates (a) SSSS and (b) CCCC [ $6 \times 6$  mesh].

panels with very thin face sheets ( $h_f/h = 0.025$ ). However, with increasing face sheet thickness, FSDT clearly over-estimates the critical temperature. The difference between FSDT and HSDT increases with skew angle. For moderately thick panels ( $a/h = 20$ ) with  $h_f/h = 0.15$ , the difference increases from about 7.4% to 18.1% as  $\Psi$  increases from  $0^\circ$  to  $45^\circ$ . For a panel with  $a/h = 10$  and  $h_f/h = 0.15$ , the difference increases from about 22.3% to 41.2% as the skew angle increases from  $0^\circ$  to  $45^\circ$ .

#### 4. Conclusions

Two  $C^0$  isoparametric finite element formulations are used for thermal buckling analysis of skew fibre-reinforced laminated composite plates and composite sandwich plates. The accuracy of the present formulations is demonstrated for isotropic plates. New results are presented for laminated anisotropic and sandwich plates with various skew geometries.

The sensitivity of the critical buckling temperature to variations in skew angle, width-to-thickness ratio and boundary conditions is studied. In general the critical temperature values increase with increase in skew angle and the increase is more pronounced in thin laminates than in thick laminates. Through-thickness shear deformation is very large in thick laminates, and this effect increases with increase in the skew angle. The results show that the differences in predictions of FSDT and HSDT are small for composite laminates. However, for sandwich panels, in comparison to HSDT,

FSDT over-estimates the critical temperature by a significant margin and the margin increases as the skew angle increases. The results presented here for both thin and thick laminates are the first of their kind and it is believed that they may serve as benchmark values for other designers and researchers to test the validity of their numerical techniques and software for similar kinds of problems.

#### Appendix A

The mid-surface strain vector,  $\bar{\epsilon}$  is expressed in terms of linear ( $\bar{\epsilon}_0$ ) and non-linear components ( $\bar{\epsilon}_L$ ) as

$$\bar{\epsilon} = \bar{\epsilon}_0 + \bar{\epsilon}_L, \tag{A.1}$$

where

$$\bar{\epsilon}_0 = \left\{ \begin{matrix} \epsilon_{x0}^0, \epsilon_{y0}^0, \epsilon_{xy0}^0, \epsilon_{x0}^*, \epsilon_{y0}^*, \epsilon_{xy0}^*, \epsilon_{x0}^{**}, \epsilon_{y0}^{**}, \epsilon_{xy0}^{**}, \epsilon_{x0}^{***}, \epsilon_{y0}^{***}, \epsilon_{xy0}^{***}, \\ \chi_{x0}^0, \chi_{y0}^0, \chi_{xy0}^0, \chi_{x0}^*, \chi_{y0}^*, \chi_{xy0}^*, \chi_{x0}^{**}, \chi_{y0}^{**}, \chi_{xy0}^{**}, \phi_{x0}^0, \phi_{y0}^0, \psi_{x0}^0, \\ \psi_{y0}^0, \phi_{x0}^*, \phi_{y0}^*, \psi_{x0}^*, \psi_{y0}^*, \phi_{x0}^{**}, \phi_{y0}^{**}, \psi_{x0}^{**}, \psi_{y0}^{**} \end{matrix} \right\}^T, \tag{A.2}$$

$$\bar{\epsilon}_L = \left\{ \begin{matrix} \epsilon_{xL}^0, \epsilon_{yL}^0, \epsilon_{xyL}^0, \epsilon_{xL}^*, \epsilon_{yL}^*, \epsilon_{xyL}^*, \epsilon_{xL}^{**}, \epsilon_{yL}^{**}, \epsilon_{xyL}^{**}, \epsilon_{xL}^{***}, \epsilon_{yL}^{***}, \epsilon_{xyL}^{***}, \\ \chi_{xL}^0, \chi_{yL}^0, \chi_{xyL}^0, \chi_{xL}^*, \chi_{yL}^*, \chi_{xyL}^*, \chi_{xL}^{**}, \chi_{yL}^{**}, \chi_{xyL}^{**}, \phi_{xL}^0, \phi_{yL}^0, \psi_{xL}^0, \\ \psi_{yL}^0, \phi_{xL}^*, \phi_{yL}^*, \psi_{xL}^*, \psi_{yL}^*, \phi_{xL}^{**}, \phi_{yL}^{**}, \psi_{xL}^{**}, \psi_{yL}^{**} \end{matrix} \right\}^T. \tag{A.3}$$

The components of linear strain vector  $\bar{\epsilon}_0$  are:

Table 6

Critical temperature parameter ( $\lambda_T$ ) for simply supported (SSSS) symmetric skew sandwich plates with composite cross-ply face sheets [ $6 \times 6$  mesh]

$a/h$	$\Psi$	Theory	$h_f/h$					
			0.025	0.050	0.075	0.100	0.150	
20	$0^\circ$	3-D Elas	0.0929	0.0855	0.0791	0.0726	0.0623	
		[13,14]						
		HSDT	0.0930	0.0860	0.0794	0.0735	0.0639	
		FSDT	0.0928	0.0868	0.0815	0.0768	0.0686	
		$15^\circ$	HSDT	0.1022	0.0939	0.0863	0.0795	0.0688
			FSDT	0.1020	0.0950	0.0890	0.0837	0.0747
	$30^\circ$	HSDT	0.1357	0.1225	0.1108	0.1010	0.0860	
		FSDT	0.1353	0.1245	0.1158	0.1085	0.0964	
	$45^\circ$	HSDT	0.2119	0.1855	0.1638	0.1464	0.1218	
		FSDT	0.2111	0.1903	0.1750	0.1629	0.1439	
	10	$0^\circ$	3-D Elas	0.3220	0.2737	0.2358	0.2072	0.1632
			HSDT	0.3231	0.2764	0.2397	0.2113	0.1732
FSDT			0.3211	0.2843	0.2592	0.2402	0.2119	
$15^\circ$			HSDT	0.3485	0.2941	0.2528	0.2216	0.1805
			FSDT	0.3462	0.3039	0.2757	0.2549	0.2245
$30^\circ$			HSDT	0.4384	0.3555	0.2975	0.2560	0.2046
		FSDT	0.4349	0.3716	0.3326	0.3053	0.2674	
$45^\circ$		HSDT	0.6252	0.4757	0.3816	0.3191	0.2478	
		FSDT	0.6187	0.5064	0.4438	0.4029	0.3499	

$$\begin{aligned}\varepsilon_{x0}^0 &= \frac{\partial u_0}{\partial x}, & \varepsilon_{y0}^0 &= \frac{\partial v_0}{\partial y}, & \varepsilon_{xy0}^0 &= \frac{\partial u_0}{\partial y}, \\ \varepsilon_{x0}^* &= \frac{\partial u_0^*}{\partial x}, & \varepsilon_{y0}^* &= \frac{\partial v_0^*}{\partial y}, & \varepsilon_{xy0}^* &= \frac{\partial u_0^*}{\partial y} + \frac{\partial v_0^*}{\partial x}, \\ \varepsilon_{x0}^{**} &= \varepsilon_{y0}^{**} = \varepsilon_{xy0}^{**} = \varepsilon_{x0}^{***} = \varepsilon_{y0}^{***} = \varepsilon_{xy0}^{***} = 0, \\ \chi_{x0}^0 &= \frac{\partial \theta_y}{\partial x}, & \chi_{y0}^0 &= -\frac{\partial \theta_x}{\partial y}, & \chi_{xy0}^0 &= \frac{\partial \theta_y}{\partial y} - \frac{\partial \theta_x}{\partial x}, \\ \chi_{x0}^* &= \frac{\partial \theta_y^*}{\partial x}, & \chi_{y0}^* &= -\frac{\partial \theta_x^*}{\partial y}, & \chi_{xy0}^* &= \frac{\partial \theta_y^*}{\partial y} - \frac{\partial \theta_x^*}{\partial x}, \\ \chi_{x0}^{**} &= \chi_{y0}^{**} = \chi_{xy0}^{**} = 0, \\ \phi_{x0}^0 &= \theta_y + \frac{\partial w_0}{\partial x}, & \phi_{y0}^0 &= -\theta_x + \frac{\partial w_0}{\partial y}, \\ \psi_{x0}^0 &= 2u_0^*, & \psi_{y0}^0 &= 2v_0^*, & \phi_{x0}^* &= 3\theta_y^*, & \phi_{y0}^* &= -3\theta_x^*, \\ \psi_{x0}^* &= \psi_{y0}^* = \phi_{x0}^{**} = \phi_{y0}^{**} = \psi_{x0}^{**} = \psi_{y0}^{**} = 0.\end{aligned}$$

The components of non-linear strain vector  $\bar{\varepsilon}_L$  are:

$$\begin{aligned}\varepsilon_{xL}^0 &= \frac{1}{2} \left( \frac{\partial u_0}{\partial x} \right)^2 + \frac{1}{2} \left( \frac{\partial v_0}{\partial x} \right)^2 + \frac{1}{2} \left( \frac{\partial w_0}{\partial x} \right)^2, \\ \varepsilon_{yL}^0 &= \frac{1}{2} \left( \frac{\partial u_0}{\partial y} \right)^2 + \frac{1}{2} \left( \frac{\partial v_0}{\partial y} \right)^2 + \frac{1}{2} \left( \frac{\partial w_0}{\partial y} \right)^2, \\ \varepsilon_{xyL}^0 &= \frac{\partial u_0}{\partial x} \frac{\partial u_0}{\partial y} + \frac{\partial v_0}{\partial x} \frac{\partial v_0}{\partial y} + \frac{\partial w_0}{\partial x} \frac{\partial w_0}{\partial y}, \\ \varepsilon_{xL}^* &= \frac{1}{2} \left( \frac{\partial \theta_x}{\partial x} \right)^2 + \frac{1}{2} \left( \frac{\partial \theta_y}{\partial x} \right)^2 + \frac{\partial u_0}{\partial x} \frac{\partial u_0^*}{\partial x} + \frac{\partial v_0}{\partial x} \frac{\partial v_0^*}{\partial x}, \\ \varepsilon_{yL}^* &= \frac{1}{2} \left( \frac{\partial \theta_x}{\partial y} \right)^2 + \frac{1}{2} \left( \frac{\partial \theta_y}{\partial y} \right)^2 + \frac{\partial u_0}{\partial y} \frac{\partial u_0^*}{\partial y} + \frac{\partial v_0}{\partial y} \frac{\partial v_0^*}{\partial y}, \\ \varepsilon_{xyL}^* &= \frac{\partial u_0}{\partial x} \frac{\partial u_0^*}{\partial y} + \frac{\partial u_0}{\partial y} \frac{\partial u_0^*}{\partial x} + \frac{\partial v_0}{\partial x} \frac{\partial v_0^*}{\partial y} + \frac{\partial v_0}{\partial y} \frac{\partial v_0^*}{\partial x} + \frac{\partial \theta_x}{\partial x} \frac{\partial \theta_x}{\partial y} \\ &\quad + \frac{\partial \theta_y}{\partial x} \frac{\partial \theta_y}{\partial y}, \\ \varepsilon_{xL}^{**} &= \frac{1}{2} \left( \frac{\partial u_0^*}{\partial x} \right)^2 + \frac{1}{2} \left( \frac{\partial v_0^*}{\partial x} \right)^2 + \frac{\partial \theta_x}{\partial x} \frac{\partial \theta_x^*}{\partial x} + \frac{\partial \theta_y}{\partial x} \frac{\partial \theta_y^*}{\partial x}, \\ \varepsilon_{yL}^{**} &= \frac{1}{2} \left( \frac{\partial u_0^*}{\partial y} \right)^2 + \frac{1}{2} \left( \frac{\partial v_0^*}{\partial y} \right)^2 + \frac{\partial \theta_x}{\partial y} \frac{\partial \theta_x^*}{\partial y} + \frac{\partial \theta_y}{\partial y} \frac{\partial \theta_y^*}{\partial y}, \\ \varepsilon_{xyL}^{**} &= \frac{\partial u_0^*}{\partial x} \frac{\partial u_0^*}{\partial y} + \frac{\partial v_0^*}{\partial x} \frac{\partial v_0^*}{\partial y} + \frac{\partial \theta_x}{\partial x} \frac{\partial \theta_x^*}{\partial y} + \frac{\partial \theta_x}{\partial y} \frac{\partial \theta_x^*}{\partial x} + \frac{\partial \theta_y}{\partial x} \frac{\partial \theta_y^*}{\partial y} \\ &\quad + \frac{\partial \theta_y}{\partial y} \frac{\partial \theta_y^*}{\partial x},\end{aligned}$$

$$\begin{aligned}\varepsilon_{xL}^{***} &= \frac{1}{2} \left( \frac{\partial \theta_x^*}{\partial x} \right)^2 + \frac{1}{2} \left( \frac{\partial \theta_y^*}{\partial x} \right)^2, \\ \varepsilon_{yL}^{***} &= \frac{1}{2} \left( \frac{\partial \theta_x^*}{\partial y} \right)^2 + \frac{1}{2} \left( \frac{\partial \theta_y^*}{\partial y} \right)^2, \\ \varepsilon_{xyL}^{***} &= \frac{\partial \theta_x^*}{\partial x} \frac{\partial \theta_x^*}{\partial y} + \frac{\partial \theta_y^*}{\partial x} \frac{\partial \theta_y^*}{\partial y}, & \chi_{xL}^0 &= \frac{\partial u_0}{\partial x} \frac{\partial \theta_y}{\partial x} - \frac{\partial v_0}{\partial x} \frac{\partial \theta_x}{\partial x}, \\ \chi_{yL}^0 &= \frac{\partial u_0}{\partial y} \frac{\partial \theta_y}{\partial y} - \frac{\partial v_0}{\partial y} \frac{\partial \theta_x}{\partial y}, \\ \chi_{xyL}^0 &= \frac{\partial u_0}{\partial x} \frac{\partial \theta_y}{\partial y} + \frac{\partial u_0}{\partial y} \frac{\partial \theta_x}{\partial x} - \frac{\partial v_0}{\partial x} \frac{\partial \theta_x}{\partial y} - \frac{\partial v_0}{\partial y} \frac{\partial \theta_x}{\partial x}, \\ \chi_{xL}^* &= \frac{\partial u_0}{\partial x} \frac{\partial \theta_y^*}{\partial x} + \frac{\partial u_0^*}{\partial x} \frac{\partial \theta_y}{\partial x} - \frac{\partial v_0}{\partial x} \frac{\partial \theta_x^*}{\partial x} - \frac{\partial v_0^*}{\partial x} \frac{\partial \theta_x}{\partial x}, \\ \chi_{yL}^* &= \frac{\partial u_0}{\partial y} \frac{\partial \theta_y^*}{\partial y} + \frac{\partial u_0^*}{\partial y} \frac{\partial \theta_y}{\partial y} - \frac{\partial v_0}{\partial y} \frac{\partial \theta_x^*}{\partial y} - \frac{\partial v_0^*}{\partial y} \frac{\partial \theta_x}{\partial y}, \\ \chi_{xyL}^* &= \frac{\partial u_0}{\partial x} \frac{\partial \theta_y^*}{\partial y} + \frac{\partial u_0^*}{\partial x} \frac{\partial \theta_y}{\partial y} + \frac{\partial u_0}{\partial y} \frac{\partial \theta_x^*}{\partial x} + \frac{\partial u_0^*}{\partial y} \frac{\partial \theta_x}{\partial x} - \frac{\partial v_0}{\partial x} \frac{\partial \theta_x^*}{\partial y} \\ &\quad - \frac{\partial v_0^*}{\partial x} \frac{\partial \theta_x}{\partial y} - \frac{\partial v_0}{\partial y} \frac{\partial \theta_x^*}{\partial x} - \frac{\partial v_0^*}{\partial y} \frac{\partial \theta_x}{\partial x}, \\ \chi_{xL}^{**} &= \frac{\partial u_0^*}{\partial x} \frac{\partial \theta_y^*}{\partial x} - \frac{\partial v_0^*}{\partial x} \frac{\partial \theta_x^*}{\partial x}, & \chi_{yL}^{**} &= \frac{\partial u_0^*}{\partial y} \frac{\partial \theta_y^*}{\partial y} - \frac{\partial v_0^*}{\partial y} \frac{\partial \theta_x^*}{\partial y}, \\ \chi_{xyL}^{**} &= \frac{\partial u_0^*}{\partial x} \frac{\partial \theta_y^*}{\partial y} + \frac{\partial u_0^*}{\partial y} \frac{\partial \theta_x^*}{\partial x} - \frac{\partial v_0^*}{\partial x} \frac{\partial \theta_x^*}{\partial y} - \frac{\partial v_0^*}{\partial y} \frac{\partial \theta_x^*}{\partial x}, \\ \phi_{xL}^0 &= \frac{\partial u_0}{\partial x} \theta_y - \frac{\partial v_0}{\partial x} \theta_x, & \phi_{yL}^0 &= \frac{\partial u_0}{\partial y} \theta_y - \frac{\partial v_0}{\partial y} \theta_x, \\ \psi_{xL}^0 &= 2u_0^* \frac{\partial u_0}{\partial x} + 2v_0^* \frac{\partial v_0}{\partial x} + \theta_x \frac{\partial \theta_x}{\partial x} + \theta_y \frac{\partial \theta_y}{\partial x}, \\ \psi_{yL}^0 &= 2u_0^* \frac{\partial u_0}{\partial y} + 2v_0^* \frac{\partial v_0}{\partial y} + \theta_x \frac{\partial \theta_x}{\partial y} + \theta_y \frac{\partial \theta_y}{\partial y}, \\ \phi_{xL}^* &= 2u_0^* \frac{\partial \theta_y}{\partial x} - 2v_0^* \frac{\partial \theta_x}{\partial x} + \theta_y \frac{\partial u_0^*}{\partial x} - \theta_x \frac{\partial v_0^*}{\partial x} + 3\theta_y^* \frac{\partial u_0}{\partial x} \\ &\quad - 3\theta_x^* \frac{\partial v_0}{\partial x}, \\ \phi_{yL}^* &= 2u_0^* \frac{\partial \theta_y}{\partial y} - 2v_0^* \frac{\partial \theta_x}{\partial y} + \theta_y \frac{\partial u_0^*}{\partial y} - \theta_x \frac{\partial v_0^*}{\partial y} + 3\theta_y^* \frac{\partial u_0}{\partial y} \\ &\quad - 3\theta_x^* \frac{\partial v_0}{\partial y}, \\ \psi_{xL}^* &= \theta_x \frac{\partial \theta_x^*}{\partial x} + \theta_y \frac{\partial \theta_y^*}{\partial x} + 2u_0^* \frac{\partial u_0^*}{\partial x} + 2v_0^* \frac{\partial v_0^*}{\partial x} + 3\theta_x^* \frac{\partial \theta_x}{\partial x} \\ &\quad + 3\theta_y^* \frac{\partial \theta_y}{\partial x}, \\ \psi_{yL}^* &= \theta_x \frac{\partial \theta_x^*}{\partial y} + \theta_y \frac{\partial \theta_y^*}{\partial y} + 2u_0^* \frac{\partial u_0^*}{\partial y} + 2v_0^* \frac{\partial v_0^*}{\partial y} + 3\theta_x^* \frac{\partial \theta_x}{\partial y} \\ &\quad + 3\theta_y^* \frac{\partial \theta_y}{\partial y},\end{aligned}$$

$$\phi_{xL}^{**} = 2u_0^* \frac{\partial \theta_y^*}{\partial x} - 2v_0^* \frac{\partial \theta_x^*}{\partial x} - 3\theta_x^* \frac{\partial v_0^*}{\partial x} + 3\theta_y^* \frac{\partial u_0^*}{\partial x},$$

$$H_i = \frac{(z_{L+1}^i - z_L^i)}{i}.$$

$$\phi_{yL}^{**} = 2u_0^* \frac{\partial \theta_y^*}{\partial y} - 2v_0^* \frac{\partial \theta_x^*}{\partial y} - 3\theta_x^* \frac{\partial v_0^*}{\partial y} + 3\theta_y^* \frac{\partial u_0^*}{\partial y},$$

$$\psi_{xL}^{**} = 3\theta_x^* \frac{\partial \theta_x^*}{\partial x} + 3\theta_y^* \frac{\partial \theta_y^*}{\partial x} \quad \psi_{yL}^{**} = 3\theta_x^* \frac{\partial \theta_x^*}{\partial y} + 3\theta_y^* \frac{\partial \theta_y^*}{\partial y}.$$

The rigidity matrices in Eq. (16) are

$$\mathbf{D}_M = \sum_{L=1}^{NL} \begin{bmatrix} Q_{ij}H_1 & Q_{ij}H_3 & Q_{ij}H_5 & Q_{ij}H_7 \\ & Q_{ij}H_5 & Q_{ij}H_7 & Q_{ij}H_9 \\ & & Q_{ij}H_9 & Q_{ij}H_{11} \\ \text{Sym.} & & & Q_{ij}H_{13} \end{bmatrix}$$

$$\mathbf{D}_C = \sum_{L=1}^{NL} \begin{bmatrix} Q_{ij}H_2 & Q_{ij}H_4 & Q_{ij}H_6 \\ Q_{ij}H_4 & Q_{ij}H_6 & Q_{ij}H_8 \\ Q_{ij}H_6 & Q_{ij}H_8 & Q_{ij}H_{10} \\ Q_{ij}H_8 & Q_{ij}H_{10} & Q_{ij}H_{12} \end{bmatrix}$$

$$\mathbf{D}_B = \sum_{L=1}^{NL} \begin{bmatrix} Q_{ij}H_3 & Q_{ij}H_5 & Q_{ij}H_7 \\ & Q_{ij}H_7 & Q_{ij}H_9 \\ \text{Sym.} & & Q_{ij}H_{11} \end{bmatrix}$$

$$\mathbf{D}_S = \sum_{L=1}^{NL} \begin{bmatrix} Q_{ml}H_1 & Q_{ml}H_2 & Q_{ml}H_3 & Q_{ml}H_4 & Q_{ml}H_5 & Q_{ml}H_6 \\ & Q_{ml}H_3 & Q_{ml}H_4 & Q_{ml}H_5 & Q_{ml}H_6 & Q_{ml}H_7 \\ & & Q_{ml}H_5 & Q_{ml}H_6 & Q_{ml}H_7 & Q_{ml}H_8 \\ & & & Q_{ml}H_7 & Q_{ml}H_8 & Q_{ml}H_9 \\ \text{Sym.} & & & & Q_{ml}H_9 & Q_{ml}H_{10} \\ & & & & & Q_{ml}H_{11} \end{bmatrix} \tag{A.4}$$

where  $i, j = 1, 2, 3$  and  $l, m = 4, 5$

### References

- [1] Reddy ARK, Palaninathan R. Buckling of laminated skew plates. *Thin-Walled Struct* 1995;22(4):241–59.
- [2] Jaunky N, Knight NF, Ambur DR. Buckling of arbitrary quadrilateral anisotropic plates. *AIAA J* 1995;33(5):938–44.
- [3] Wang S. Buckling analysis of skew fibre-reinforced composite laminates based on first-order shear deformation plate theory. *Compos Struct* 1997;37(1):5–19.
- [4] Babu CS, Kant T. Two shear deformable finite element models for buckling analysis of skew fibre-reinforced composite and sandwich panels. *Compos Struct* 1999;46(2):115–24.
- [5] Prabhu MSS, Durvasula S. Elastic stability of thermally stressed clamped-clamped skew plates. *ASME J Appl Mech* 1974;41(3): 820–1.
- [6] Prabhu MSS, Durvasula S. Thermal buckling of restrained skew plates. *ASCE J Eng Mech* 1974;100(6):1292–5.
- [7] Prabhu MSS, Durvasula S. Thermal post-buckling characteristics of clamped skew plates. *Comput Struct* 1976;6(3):177–85.
- [8] Kant T. Numerical analysis of thick plates. *Comput Meth Appl Mech Eng* 1982;31(1):1–18.
- [9] Kant T, Owen DRJ, Zienkiewicz OC. A refined higher-order  $C^0$  plate bending element. *Comput Struct* 1982;15(2):177–83.
- [10] Kant T, Pandya BN. A simple finite element formulation of a higher-order theory for unsymmetrically laminated composite plates. *Compos Struct* 1988;9(3):215–46.
- [11] Zienkiewicz OC, Taylor RL. *The finite element method*. 4th ed., vol. 1. Singapore: McGraw-Hill, 1989.
- [12] Noor AK, Burton WS. Three-dimensional solutions for thermal buckling of multilayered anisotropic plates. *ASCE J Eng Mech* 1992;118(4):683–701.
- [13] Noor AK, Peters JM, Burton WS. Three-dimensional solutions for initially stressed structural sandwiches. *ASCE J Eng Mech* 1994;120(2):284–303.
- [14] Noor AK, Burton WS, Bert CW. Computational models for sandwich panels and shells. *Appl Mech Rev* 1996;49(3):155–99.